J Nanostruct 16(1): 849-860, Winter 2026

RESEARCH PAPER

Synthesis of MoS_2 Nanopowder Based on the Design of the Experiment with Taguchi

*Mehdi Abdolmaleki [1] *, Younes Hanifehpour [1], Somayeh Ahmadiyeh [2], Saman Golmohamadi [3]*

[1] *Department of Chemistry, Sayyed Jamaleddin Asadabadi University, Asadabad 6541853096, Iran*

[2] *Department of Materials Engineering, Faculty of Mechanical Engineering, University of Tabriz, Tabriz, Iran*

[3] *Department of Chemistry, Tuyserkan Branch, Islamic Azad University, Tuyserkan, Iran*

ARTICLE INFO

Article History:
Received 29 July 2025
Accepted 11 December 2025
Published 01 January 2026

Keywords:
Molybdenum disulfide
Nanopowder
Solvothermal method
Taguchi

ABSTRACT

Molybdenum disulfide nanopowders (MoS_2) have been successfully prepared via solvothermal method using different precursors of molybdenum and sulfur, at different times and temperatures. According to L_9 Taguchi orthogonal design, synthesizing process parameters of MoS_2 powder are optimized for producing smaller powders with four process parameters, viz., and precursor of molybdenum, the precursor of sulfur, different times, and reaction temperatures. The prepared MoS_2 powders were examined via scanning electron microscopy (SEM) with energy-dispersive X-ray spectroscopy (EDS), Fourier transform infrared spectrometer (FTIR), X-ray diffraction (XRD), and differential thermal analysis (DTA). SEM measurements were conducted to determine the grain size of the powders. According to the study conducted by Taguchi, the Mo precursor and reaction temperature had the most substantial effect on the particle size of MoS_2. Finally, optimum conditions were achieved as follows: molybdic oxide as Mo precursor, sodium sulfide as a sulfur source, 72 h, and 150 °C as reaction time and temperature. The hexagonal 2H-MoS_2 can be easily indexed for the XRD pattern of the sample synthesized from optimum conditions. FTIR spectrum of the optimized MoS_2 showed the band at 469 cm^{-1} corresponds to the ν (Mo-S) and its SEM image exhibited the MoS_2 nanolamellar with a diameter of 40-90 nm.

How to cite this article
Abdolmaleki M., Hanifehpour Y., Ahmadiyeh S., Golmohamadi S. Synthesis of MoS_2 Nanopowder Based on the Design of the Experiment with Taguchi. J Nanostruct, 2026; 16(1):849-860. DOI: 10.22052/JNS.2026.01.075

INTRODUCTION

Transition metal dichalcogenides MX_2 (M = Mo, W, Nb and Ta, X = S, Se), in which a layered structure is constituted in comparison to graphite, has recently generated considerable interest. The reason for this increasing popularity is their promising applications and prominent characteristics [1, 2]. Nanoparticles of many inorganic compounds, including MoS_2, WS_2 have not enough stability against folded in comparison to graphite, and are capable of adopting fullerene-like and nanotubular structures [3]. Their synthesis has recently received increasing attention since they can be potentially employed in the realm of catalysis [4, 5], lubrication [6-8], electrochemistry [9, 10], and as host materials

* *Corresponding Author Email: abdolmaleki11@yahoo.com*

in intercalation chemistry [11, 12]. Since the characteristics of materials are affected by its shape and size, for example, nanoscale MoS_2 has more favorable characteristics in comparison to normal MoS_2, including much greater particular surface areas, considerable absorbing ability, particularly hydro-desulfurization (HDS) catalyzing capability [13, 14]. Thus, more attempts have been made in the synthesis of several MoS_2 nanoscales having distinctive characteristics and particular morphologies. There have been various MoS_2 structures, such as inorganic fullerene [15, 16], micro and nano flowers [17, 18], nanotubes [19-21], nanorods [22, 23], nanowires [24, 25], nanolamellar [26] and core-shell structures [27, 28].

There have been several preparation approaches for various nanostructural materials, including chemical vapor deposition, spray pyrolysis, sol-gel processing, metathesis reactions, two-step electrochemical synthesis, co-precipitation, sonochemical synthesis, and so on [29-32]. The first discovery of spherical fullerene-like nanoparticles of MoS_2 and WS_2 nanotubes was made by Tenne et al. in 1992 [33]. MoS_2 nanotubes were achieved by Rao et al. via simple heating MoS_3 under high temperature in a stream of hydrogen. An attempt was made by Zelenski et al. to synthesize tubules and fibers of MoS_2 using the thermal decomposition of ammonium thiomolybdate precursors at 450 °C [34]. The hydrothermal approach was utilized by Yumei et al. to synthesize MoS_2 nanospheres and nanorods [23, 35]. As water is applied as a reaction solvent instead of organics, hydrothermal synthesis as an environmentally friendly method has received great attention. As this approach is a simple, low-cost, and high-efficiency approach, it has been extensively applied for the preparation of nanostructures [36].

In this study, the Taguchi approach is applied reports to specify the optimum synthesizing process factors to achieve molybdenum disulfide powder with nano metric scale. According to the Taguchi orthogonal, four design factors of precursor of molybdenum, precursor of sulfur, duration, and the temperature of reaction are involved in the experiments on the morphology of the MoS_2. Three levels of maximum, minimum, and middle levels are considered for the selected parameters.

MATERIALS AND METHODS

Materials

The applied chemicals and materials used during the tests were listed in the following: sodium molybdate dihydrate ($Na_2MoO_4{\cdot}2H_2O$, 99%, Merck), ammonium heptamolybdate tetrahydrate ($(NH_4)_6Mo_7O_{24}{\cdot}4H_2O$, 99%, Merck), molybdic oxide (MoO_3, 99%, Merck), potassium thiocyanate (KSCN, 99%, Merck), thioacetamide (C_2H_5NS, 99%, Aldrich), sodium sulfide (Na_2S, 99%, Merck), doubly distilled water was used for the preparation of the solutions.

Synthesis and characterization of MoS_2 powders

The synthesis of MoS_2 nanopowders was classified divided into two phases. A typical procedure was as follows. In the first trail, Mo source ($Na_2MoO_4{\cdot}2H_2O$, $(NH_4)_6Mo_7O_{24}{\cdot}4H_2O$or MoO_3) were put into a Teflon-lined autoclave with a capacity of 100 ml. The autoclave was then filled with 20 ml distilled water and 40 ml ethanol. A stainless steel tank was used to seal the autoclave, and it was equilibrated at 50 °C for 4 h. Secondly, the sulfur precursor (KSCN, Na_2S, or C_2H_5NS) was put into the autoclave, and 5 mL distilled water and 10 mL ethanol was added to it. The mole ratio of Mo precursors to the sulfur source is 1:2. The autoclave was kept at 150, 200, and 250 °C respectively for 24 h, 48 h, and 72 h, and the temperature was naturally reduced to room temperature.

Centrifugation method was conducted to retrieve the powder from the solution, and it was washed by ethanol and distilled water for several times to eliminate the reactants residue, and finally dried in air.

A field emission scanning electron microscope (FESEM) model TESCAN MIRA3 electron microscopy was employed for determining the particle morphology and the powders size. Furthermore, energy dispersive X-ray spectroscopy (EDS) experiments carried out in the SEM were also used to specify the composition of the synthesized powders.

After drying, the synthesized powders were analyzed by XRD (X-Ray Diffractometer APD 2000, Cu-kα radiation) and thermo gravimetric analysis and differential thermal analysis (TG/DTA) (Pyris diamond TG/DTA, Perkin Elmer). TG/DTA of powders was performed from 30 to 1100 °C at a scan rate of 10 °C /min under inert nitrogen

atmosphere. The Fourier transform infrared spectrum of the samples (FTIR) was collected by PerkinElmer Spectrum Two FT-IR spectrometer.

TAGUCHI DESIGN OF EXPERIMENT

Design of orthogonal array and signal-to-noise analysis

Taguchi method [37, 38] is accounted for as an effective technique to design the high-quality systems according to orthogonal array trials in which much-reduced variance for the trials and an optimum setting of the procedure control factors are provided. In this approach, the design of experiments (DOE) is integrated with the parametric optimization of the procedure by which favorable results are obtained [37, 38]. Four factors (type of molybdenum precursor, type of sulfur precursor, time, and reaction temperature) selected with three levels are demonstrated in Table 1.

The levels and parameterswere appliedtodesignan orthogonal array L_9 (3^4) for the trials. To make sure the reliability of experimental data is achieved for a signal-to-noise (S/N) analysis,the nine Taguchi experiments were carried outtwice. Various repetitions are integrated into one value bt the S/N ratio to reflect the amount of variation present which is described as the ratio of the average(signal) to the standard deviation (noise). There have been three types of S/N ratios [38]: lower is best (LB), higher is best (HB) and nominal is best (NB). In this survey, particle size is consideredas a characteristic value. The parameters optimization was conducted with an objective for minimizing the particle size. Hence, the S/N ratio for LB characteristics was adopted and measured in the following:

$$\frac{S}{N_{LB}} = -10\log\left(\frac{1}{n}\sum_{i=1}^{n} Q_i^2\right) \quad (1)$$

Where n and Q_i are the repetition number of each trial for design factors under the same condition and the particle size of an individual evaluation at the i th experiment. The optimal level, considered as the maximum S/N ratio compared to all the parameters levels, was measured after the average S/N ratios specified and plotted at each level for different parameters.

Table 1. Design factors and levels.

Variable	Level 1	Level 2	Level 3
A: Mo source type	$Na_2MoO_4{\cdot}2H_2O$	$(NH_4)_6Mo_7O_{24}{\cdot}4H_2O$	MoO_3
B: S source type	KSCN	Na_2S	C_2H_5NS
C: reaction time (h)	24	48	72
D: reaction temperature (°C)	150	200	250

Table 2. L9 OA with design factors and their levels.

Experiment	A	B	C	D	Particle size (nm)	
					Test 1	Test 2
1	1	1	1	1	150	200
2	1	2	2	2	200	250
3	1	3	3	3	700	800
4	2	1	2	3	850	950
5	2	2	3	1	50	70
6	2	3	1	2	250	300
7	3	1	3	2	70	100
8	3	2	1	3	90	130
9	3	3	2	1	100	150

Analysis of variance (ANOVA)

ANOVA is a statistical approach by which some major conclusions can be inferred according to the analysis of the experimental data. Identifying the significance level of factor(s) influence and the contribution of factors to the particle size of powders can be relatively simple after the analysis. The total variability of the response is divided into contributions of each of the parameters and the error [39-41]. According to the ANOVA table, SS, D, V, SS', and P is the sum of the square, the degree of freedom, the variance, the corrected sum of the square, and the percentage contribution of each parameter, respectively [38].

RESULTS AND DISCUSSION

Particle size studies

To calculate the grain size of the powders, SEM measurements were performed. Table 2 presents the structure of the Taguchi's orthogonal array design as well as the grain size measurements results for various powders. The particle size of powders produced from different experiments is in the range of 50-950 nm.

Determination of optimal levels

According to Eq. 1, two grain size measurements were converted into an S/N ratio for each experiment. A comparison made between the calculated mean S/N ratios and the data of particle size is tabulated in Table 3.

According to Table 4 which is named the S/N response table for grain size, the average S/N ratio for each level of the parameters A, B, C, and D is shown. Furthermore, it shows the total average S/N ratio for the 9 trials.

The mean value of the adopted properties for the level of each parameter is tabulated in the response Table 4. This table also shows ranks according to Delta statistics in which a comparison between the relative magnitudes of effects is made. The maximum average value of each factor minus the minimum average value of the same is defined as the Delta statistic. Ranks are considered according to Delta values; rank 1 is related to the maximum Delta value, rank 2 to

Table 3. The S/N ratios.

Experiment	Particle size (nm)		S/N ratio
	Test 1	Test 2	
1	150	200	-44.949
2	200	250	-47.097
3	700	800	-57.521
4	850	950	-59.099
5	50	70	-35.683
6	250	300	-48.823
7	70	100	-38.722
8	90	130	-40.97
9	100	150	-40.109

Table 4. Response table of mean S/N ratio.

Level	Factor			
	A	B	C	D
1	-49.856	-47.59	-44.914	-40.914
2	-47.868	-41.25	-49.435	-44.881
3	-39.994	-49.484	-43.975	-52.53
Delta	9.862	8.234	5.46	11.616
Rank	2	3	4	1

The total mean S/N ratio = -46.108

the second-highest Delta value, and so on. Figs 1 and 2, demonstrate the plots of the main effect and interaction effect between the parameters. According to the plot in Fig. 1, a particular factor has no substantial effect if the line for the factor is near horizontal [37-40]. Therefore, it can be seen that parameters D (reaction temperature) and A (Mo source type) have the most substantial effect while parameters B (S source type) and C (reaction time) have relatively less significant influence (Fig. 1).

On the other hand, according to the plot Fig. 2, interaction occurs if the lines are non-parallel, and strong interaction occurs between factors if the lines cross [37-40]. Therefore, it is obvious that there is a strong interaction between the factors A and B, whereas there is a moderate interaction between the factors B and D and weak interaction between B and C. Therefore, according to the conducted analysis, A (type of Mo precursor) and D (reaction temperature) have the most significant effect on particle size. Moreover, the optimal process parameter combination for producing of MoS_2 nanopowders is obtained as A3B2C3D1 (type of Mo precursor = MoO_3, S source type = Na_2S, reaction time = 72 h, reaction temperature = 150 ºC).

The mechanism for the formation of MoS_2 powder includes two stages:(1) during the solvothermal phase, it is possible for Mo(VI) to decrease to Mo(IV) by increasing the temperature and pressure, and it then reacts with S; (2) then initial formed MoS_2 might instantly aggregate to form small particles.

For example, the overall reaction of synthesizing of MoS_2 powder can be expressed when Na_2S as

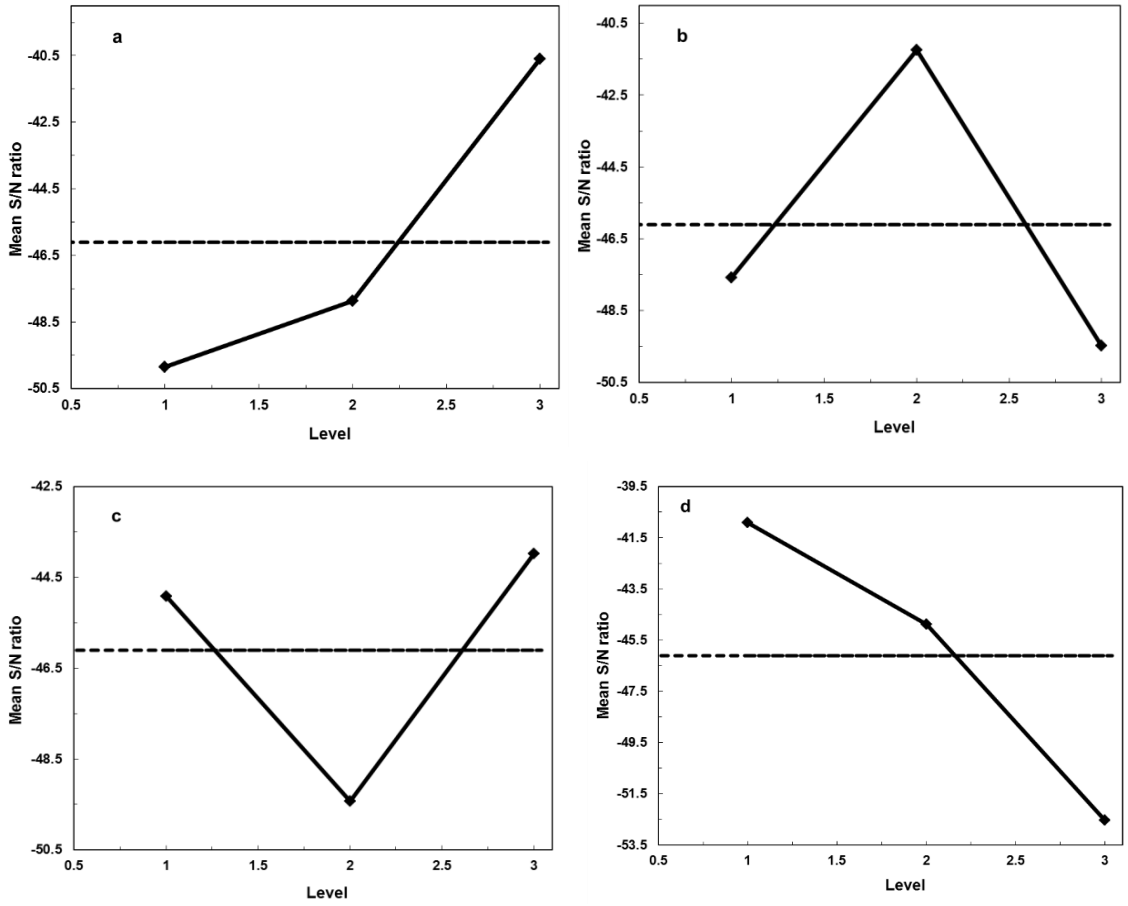

Fig. 1. Effect of (a) Mo source type, (b) S source type, (c) reaction time and (d) reaction temperature on mean S/N ratio.

the sulfur source is:

$$2MoO_3+4Na_2S+4H_2O \rightarrow 2MoS_2+O_2+8NaOH$$

Factor contributions

The variance (ANOVA) analysis can be conducted to determine the contribution of each parameter on the grain size. Table 5 summarized the obtained results of the analysis. According to the data tabulated in Table 5, the contribution of the four factors, i.e. reaction temperature, type of molybdenum precursor, type of sulfur precursor, and time of reaction is 40.669%, 27.692%, 21.695%,

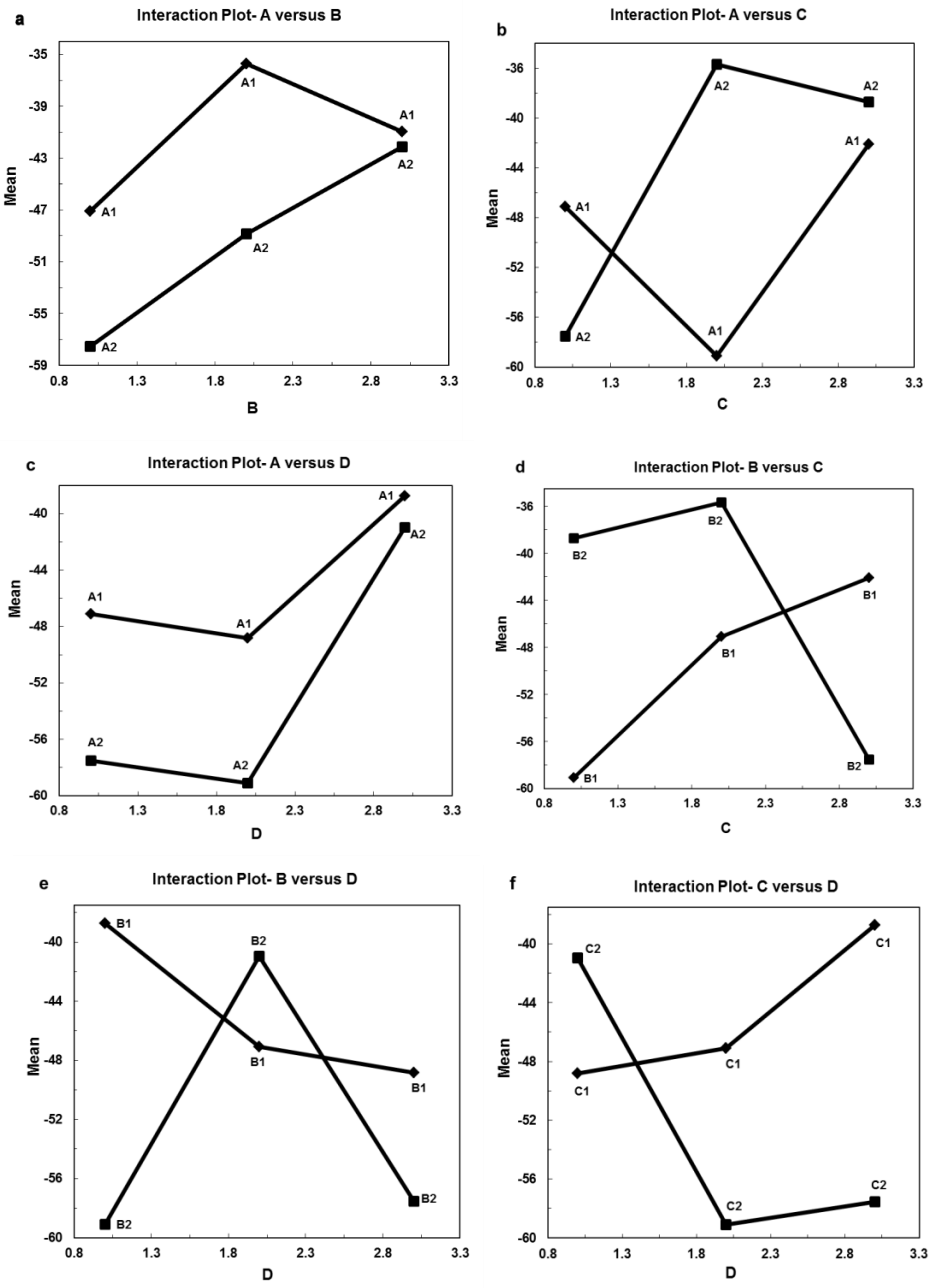

Fig. 2. Plots of interaction effect of parameters for particle size.

and 9.941%, respectively. It can be seen that the reaction temperature and type of molybdenum precursor have the most significant effect on the particle size of MoS_2 powders compared to the adopted factors.

Confirmation run

The confirmation experiment for producing MoS_2 nanopowder was carried out via setting the experimental condition of the four parameters as follows: MoO_3 for Mo source, Na_2S for S source, 72 h, and 150 °C for time and reaction temperature, respectively. Fig. 3 illustrates the SEM micrographs of the MoS_2 powder synthesized at the optimal combination of the factors A, B, C, and D. The SEM image of MoS_2 synthesized from optimum condition shows sheet like structure so that each particle is composed of multiple lamellar sheets (Fig. 3). The particle size is varying from approximately 20-90 nm. According to the chemical analysis via EDS, the existence of Mo and S is evident (elements of MoS_2).

Moreover, based on the peaks quantification, the atomic ratio of S to Mo is 1.92, which has a very close value to the stoichiometric MoS_2 (Fig. 4). The Au signal is aroused from the gold coating of samples before the SEM/EDS test.

Fig. 5 shows the crystalline nature of MoS_2 sample prepared at the optimum condition with an XRD pattern indexed at 14.81°, 32.41°, 39.5°,

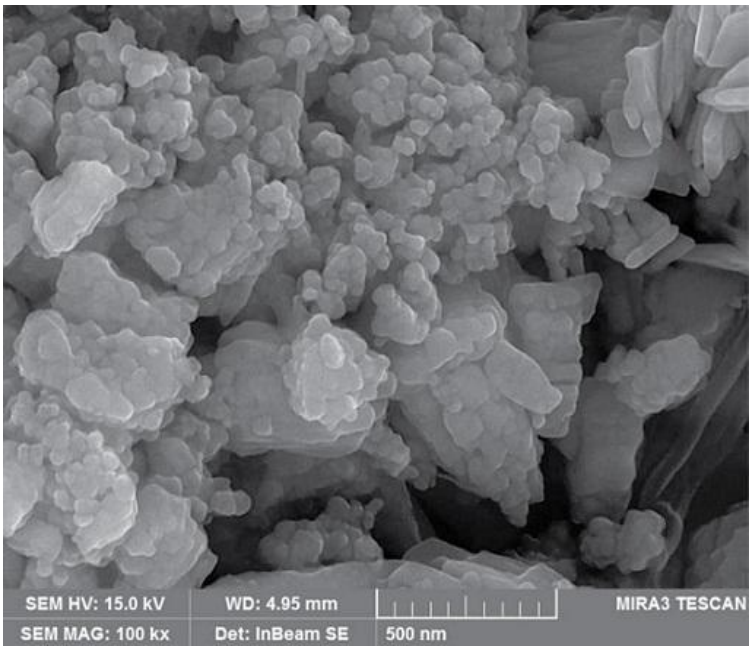

Fig. 3. SEM image of the MoS_2 prepared at optimal conditions.

Table 5. Results of the ANOVA for particle size.

Factors	Degree of freedom (D)	Sum of squares (SS)	Variance (V)	Corrected sum of squares (SS')	% Contribution (P)	Rank
A	2	142.436	71.218	142.436	27.692	2
B	2	111.592	55.796	111.592	21.695	3
C	2	51.132	25.566	51.132	9.941	4
D	2	209.183	104.591	209.183	40.669	1
Error	0	0	0	0	0	
Total	8	514.345			100%	

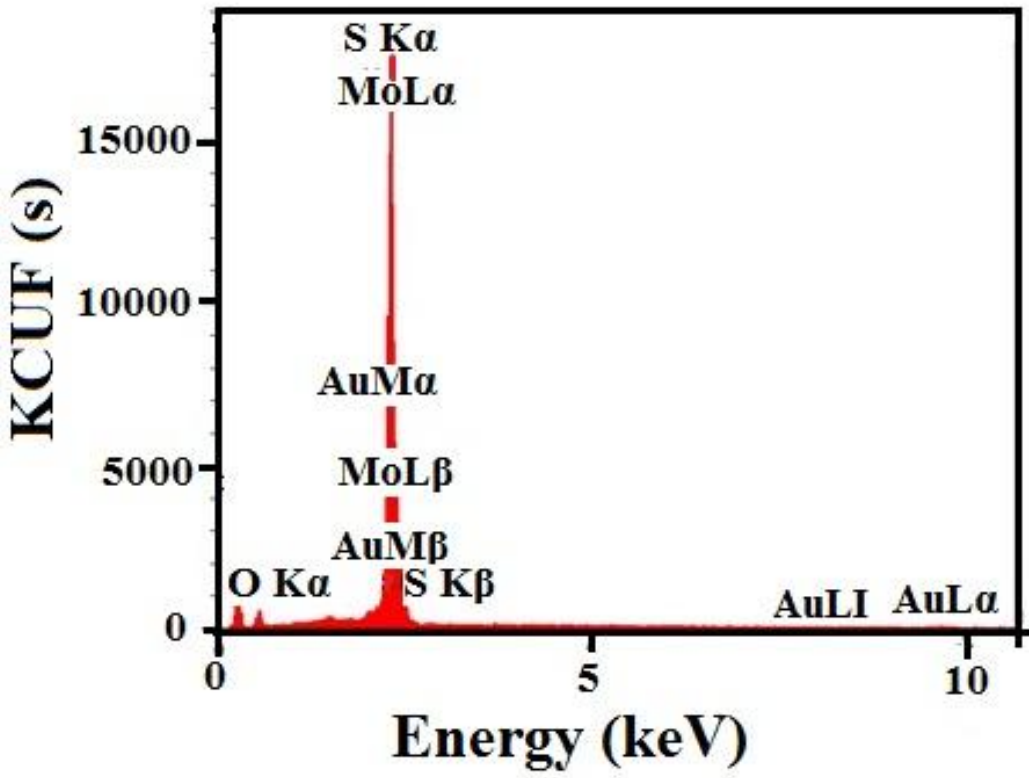

Fig. 4. EDS pattern of the MoS_2 prepared at optimal conditions.

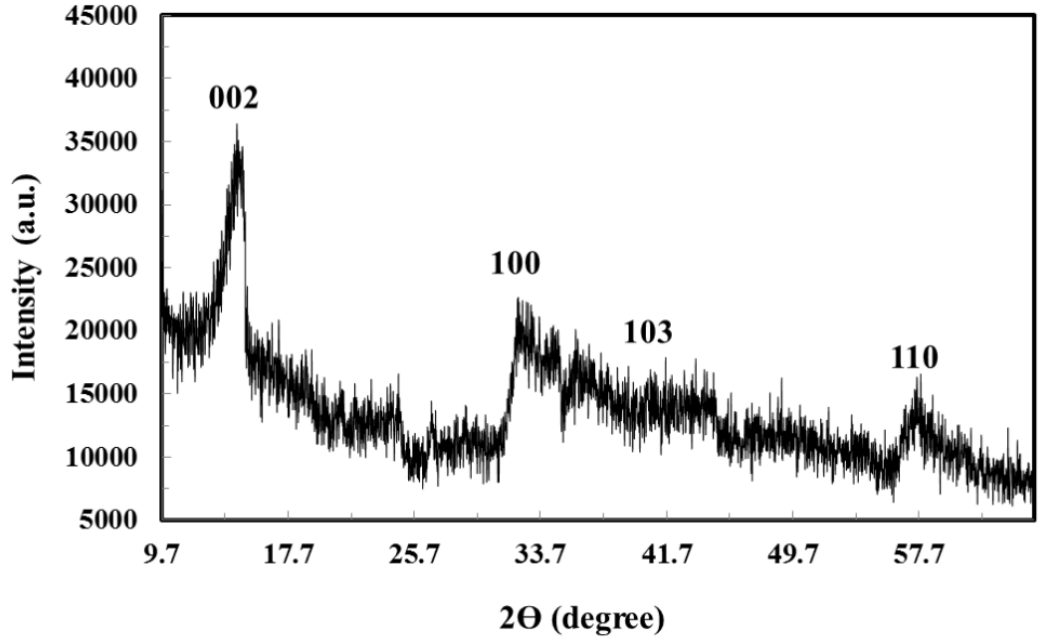

Fig. 5. XRD spectrum of the MoS_2 prepared at optimal conditions.

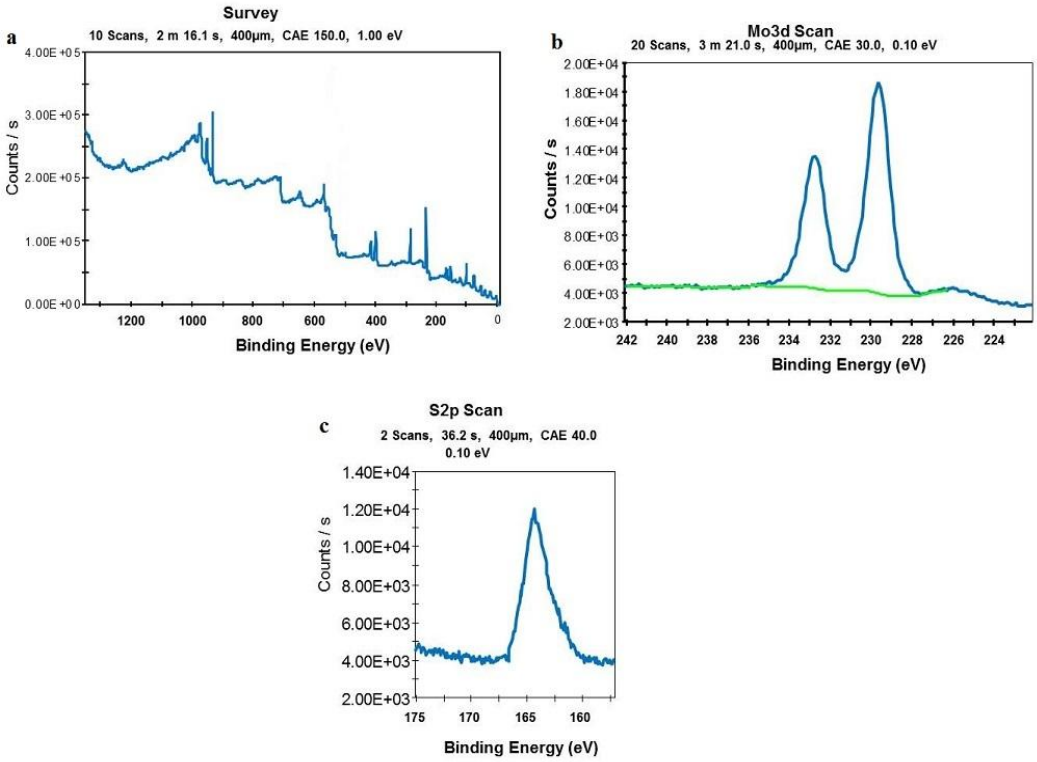

Fig. 6. XPS spectrum of the MoS_2 prepared at optimal conditions.

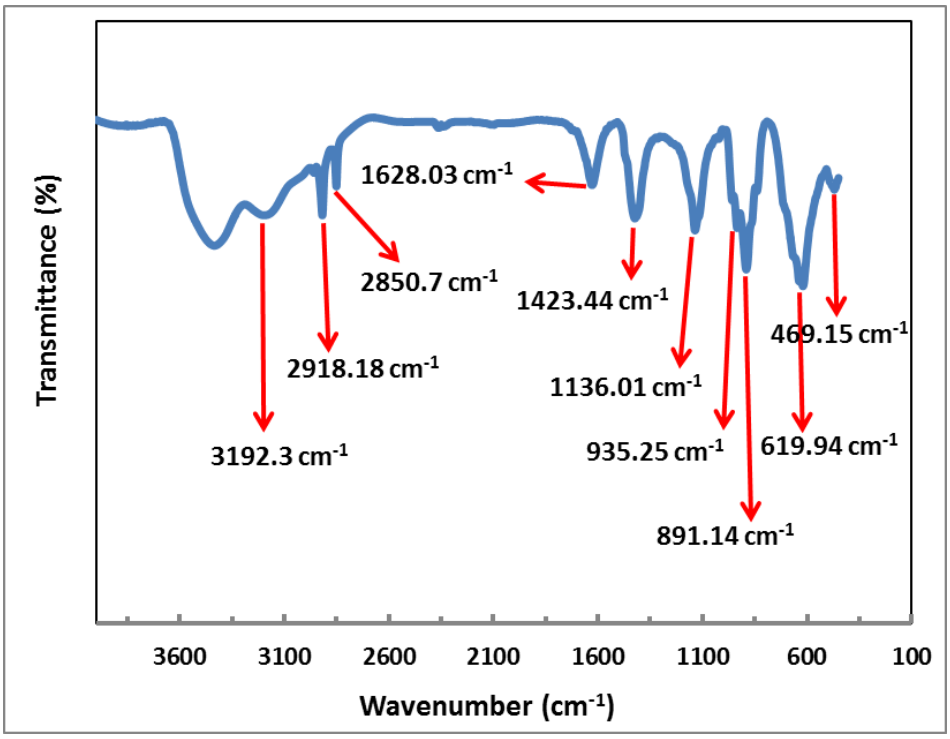

Fig. 7. FTIR spectrum of MoS_2 nanolamellar prepared at optimal conditions.

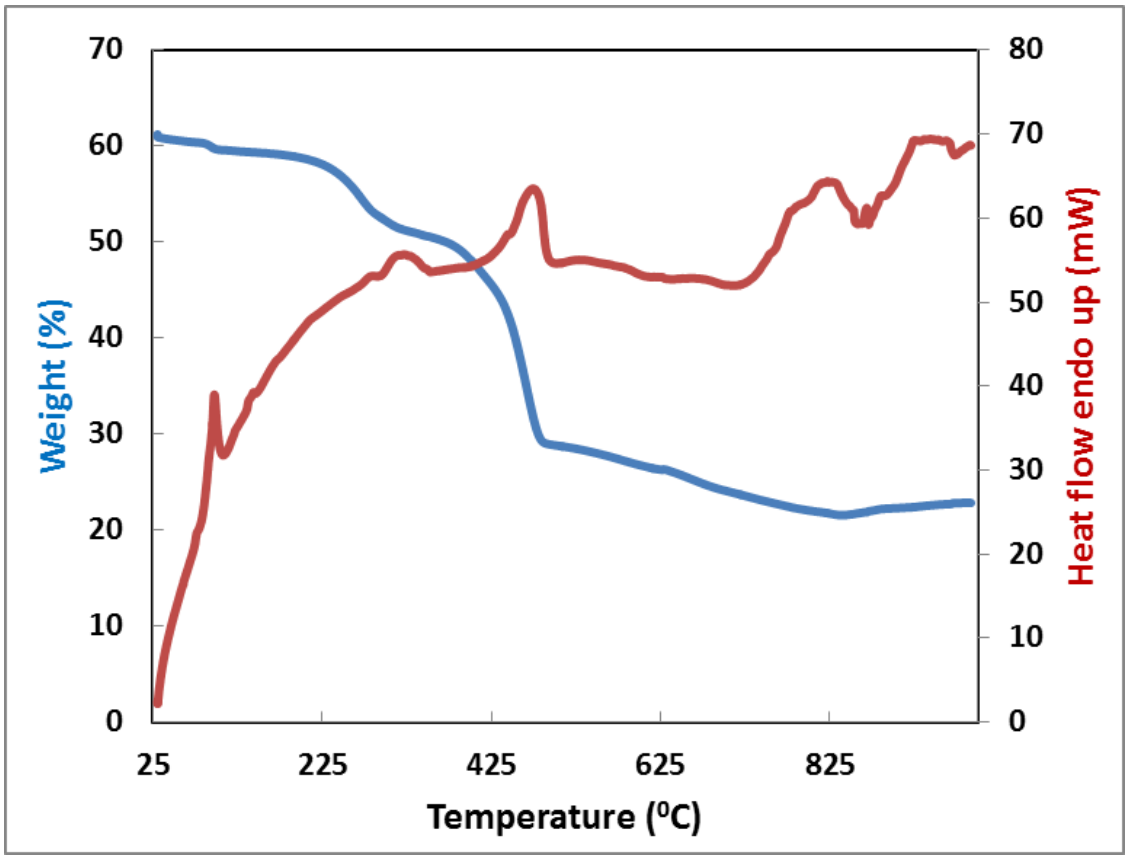

Fig. 8. TGA-DTA results for nanolamellar MoS_2.

and 58°corresponding to the (002), (100), (103), and (110) crystal planes of the MoS_2. In general, the hexagonal 2H-MoS_2 can be easily indexed for all the reflections. The presence of the 002 diffraction at 2θ = 14.81° indicates that the sample should be a stacking of single sheets of MoS_2 or multiple lamellar sheets [16, 23, 42, 43]. This is in proper agreement with the SEM results.

XPS analysis was used to measure binding energies of Mo and S atom. As shown in Fig. 6b, two asymmetric peaks centred at 229.4 eV and 232.6 eV are due to the transitions of Mo $3d_{5/2}$ and $3d3_{/2}$, respectively. The S2p curve of MoS_2 indicates a strong peak at around 163.9 eV, which is attributed to the coordination of Sulphur and Mo atoms in the structure of MoS_2 (Fig. 6c) [44].

Fig. 7 shows the FTIR spectrum of MoS_2 powder synthesized in optimum condition in the range 400-4000 cm^{-1} at room temperature. As seen in this image, the strong band at 469.15 cm^{-1} assigned to ν(Mo-S). Also, we assign the band at 619.94 and 891.14 cm^{-1} to ν(O-Mo-O) vibrations and 935.25 cm^{-1} to ν(Mo=O) vibrations.

Heat low and gravimetric curves for MoS_2 produced in optimum condition are shown in Fig. 8. Nanolamellar optimum MoS_2 is stable up to 400 °C. The more heating of this sample up to 500 °C due to prime disulfide decomposition into molybdenum and sulfur causes a high weight loss (36%).

These results support MoS_2 powder have been synthesized successfully.

CONCLUSION

Taguchi's experimental design method was utilized to perform the experiments for studying the effects of process factors, including molybdenum precursor, sulfur source, and the reaction temperature and duration on the morphology of the MoS_2 powder. The Taguchi orthogonal array is applied to the optimization of the process factors of the synthesis of MoS_2

with nano metric size. It is evident that reaction temperature and Mo precursor have a major effect on synthesizing MoS_2 nanopowder. The optimized values for producing MoS_2 particles with nano sizes are obtained as molybdenum precursor = MoO_3, sulfur source= Na_2S, reaction temperature = 150 ºC, reaction time= 72 h. SEM image of MoS_2 sample synthesized at optimal conditions exhibited the lamellar structure composed of discrete MoS_2 nanoparticles with an average crystallite size of about 55 nm. The XRD pattern confirmed the crystal diffraction planes of hexagonal MoS_2. FTIR result confirmed Mo-S vibration peak around 470 cm^{-1}. In general, the results of SEM/EDS, XRD, TGA, and FTIR analyses exhibited that nanolamellar MoS_2 nanostructures synthesized by a facile hydrothermal route in according to optimal condition proposed by Taguchi design, successfully. And, the next research work will be focused on the investigation of the super-capacitor performance of them.

ACKNOWLEDGEMENTS

This research was supported by the Sayyed Jamaleddin Asadabadi University, Asadabad, Iran. Also, the authors would like to acknowledge the financial support of the Office in Charge of Research of Iranian Nanotechnology Society and the financial support of the Office of Vice chancellor in charge of research of Sayyed Jamaleddin Asadabadi University.

CONFLICT OF INTEREST

The authors declare that there is no conflict of interests regarding the publication of this manuscript.

REFERENCES

1. Tonti D, Varsano F, Decker F, Ballif C, Regula M, Remškar M. Preparation and Photoelectrochemistry of Semiconducting WS_2 Thin Films. The Journal of Physical Chemistry B. 1997;101(14):2485-2490.
2. Tenne R. Advances in the Synthesis of Inorganic Nanotubes and Fullerene-Like Nanoparticles. Angew Chem Int Ed. 2003;42(42):5124-5132.
3. Wiesel I, Arbel H, Albu-Yaron A, Popovitz-Biro R, Gordon JM, Feuermann D, et al. Synthesis of WS_2 and MoS_2 fullerene-like nanoparticles from solid precursors. Nano Research. 2009;2(5):416-424.
4. Li Y, Wang H, Xie L, Liang Y, Hong G, Dai H. MoS_2 Nanoparticles Grown on Graphene: An Advanced Catalyst for the Hydrogen Evolution Reaction. Journal of the American Chemical Society. 2011;133(19):7296-7299.
5. Liu H, Lv T, Zhu C, Su X, Zhu Z. Efficient synthesis of MoS_2 nanoparticles modified TiO_2 nanobelts with enhanced visible-light-driven photocatalytic activity. J Mol Catal A: Chem. 2015;396:136-142.
6. Xu Z, Lou W, Zhao G, Zhao Q, Xu N, Hao J, et al. Preparation of WS_2 nanocomposites via mussel-inspired chemistry and their enhanced dispersion stability and tribological performance in polyalkylene glycol. J Dispersion Sci Technol. 2018;40(5):737-744.
7. Tang H, Li C, Yang X, Mo C, Cao K, Yan F. Synthesis and tribological properties of $NbSe_3$ nanofibers and $NbSe_2$ microsheets. Cryst Res Technol. 2011;46(4):400-404.
8. Rapoport L, Fleischer N, Tenne R. Applications of WS2(MoS_2) inorganic nanotubes and fullerene-like nanoparticles for solid lubrication and for structural nanocomposites. J Mater Chem. 2005;15(18):1782.
9. Li D, Zhang C, Du G, Zeng R, Wang S, Guo Z, et al. Enhanced Electrochemical Performance of MoS_2 for Lithium Ion Batteries by Simple Chemical Lithiation. J Chin Chem Soc. 2012;59(10):1196-1200.
10. Xiao J, Choi D, Cosimbescu L, Koech P, Liu J, Lemmon JP. Exfoliated MoS_2 Nanocomposite as an Anode Material for Lithium Ion Batteries. Chem Mater. 2010;22(16):4522-4524.
11. Benavente E. Intercalation chemistry of molybdenum disulfide. Coord Chem Rev. 2002;224(1-2):87-109.
12. Santa Ana MA, Mirabal N, Benavente E, Gómez-Romero P, González G. Electrochemical behavior of lithium intercalated in a molybdenum disulfide-crown ether nanocomposite. Electrochimica Acta. 2007;53(4):1432-1438.
13. Moses PG, Hinnemann B, Topsøe H, Nørskov JK. The effect of Co-promotion on MoS_2 catalysts for hydrodesulfurization of thiophene: A density functional study. J Catal. 2009;268(2):201-208.
14. Liu L-h, Liu S-q, Yin H-l, Liu Y-q, Liu C-g. Hydrogen spillover effect between Ni_2P and MoS_2 catalysts in hydrodesulfurization of dibenzothiophene. Journal of Fuel Chemistry and Technology. 2015;43(6):708-713.
15. Hu JJ, Sanders JH, Zabinski JS. Synthesis and microstructural characterization of inorganic fullerene-like MoS_2 and graphite- MoS_2 hybrid nanoparticles. J Mater Res. 2006;21(4):1033-1040.
16. Zou TZ, Tu JP, Huang HD, Lai DM, Zhang LL, He DN. Preparation and Tribological Properties of Inorganic Fullerene-like MoS_2. Adv Eng Mater. 2006;8(4):289-293.
17. Zhang X, Xue M, Yang X, Luo G, Yang F. Hydrothermal synthesis and tribological properties of $MoSe_2$ nanoflowers. Micro and Nano Letters. 2015;10(7):339-342.
18. Hu Z, Wang L, Zhang K, Wang J, Cheng F, Tao Z, et al. MoS_2 Nanoflowers with Expanded Interlayers as High-Performance Anodes for Sodium-Ion Batteries. Angew Chem Int Ed. 2014;53(47):12794-12798.
19. Nath M, Govindaraj A, Rao CNR. Simple Synthesis of MoS_2 and WS_2 Nanotubes. Adv Mater. 2001;13(4):283-286.
20. Chen J, Kuriyama N, Yuan H, Takeshita HT, Sakai T. Electrochemical Hydrogen Storage in MoS_2 Nanotubes. Journal of the American Chemical Society. 2001;123(47):11813-11814.
21. Seifert G, Jungnickel G, Frauenheim T, Terrones H, Terrones M. METAL Chalcogenide Nanotubes - Structure and Electronic Properties. Cluster and Nanostructure Interfaces; 2000/08: WORLD SCIENTIFIC; 2000. p. 393-396.
22. Lin H, Chen X, Li H, Yang M, Qi Y. Hydrothermal synthesis and characterization of MoS_2 nanorods. Mater Lett. 2010;64(15):1748-1750.
23. Tian Y, Zhao J, Fu W, Liu Y, Zhu Y, Wang Z. A facile route to

synthesis of MoS_2 nanorods. Mater Lett. 2005;59(27):3452-3455.
24. Li W-J, Shi E-W, Ko J-M, Chen Z-z, Ogino H, Fukuda T. Hydrothermal synthesis of MoS_2 nanowires. J Cryst Growth. 2003;250(3-4):418-422.
25. Chen Z, Cummins D, Reinecke BN, Clark E, Sunkara MK, Jaramillo TF. Core–shell MoO_3– MoS_2 Nanowires for Hydrogen Evolution: A Functional Design for Electrocatalytic Materials. Nano Lett. 2011;11(10):4168-4175.
26. Yang T, Feng X, Tang Q, Yang W, Fang J, Wang G, et al. A facile method to prepare MoS_2 with nanolameller-like morphology. J Alloys Compd. 2011;509(24):L236-L238.
27. Xing Z, Yang X, Asiri AM, Sun X. Three-Dimensional Structures of MoS_2@Ni Core/Shell Nanosheets Array toward Synergetic Electrocatalytic Water Splitting. ACS Applied Materials and Interfaces. 2016;8(23):14521-14526.
28. Yang L, Guo S, Li X. Au nanoparticles@MoS_2 core-shell structures with moderate MoS 2 coverage for efficient photocatalytic water splitting. J Alloys Compd. 2017;706:82-88.
29. Close MR, Petersen JL, Kugler EL. Synthesis and Characterization of Nanoscale Molybdenum Sulfide Catalysts by Controlled Gas Phase Decomposition of $Mo(CO)_6$ and H_2S. Inorganic Chemistry. 1999;38(7):1535-1542.
30. Bonneau PR, Jarvis RF, Kaner RB. Rapid solid-state synthesis of materials from molybdenum disulphide to refractories. Nature. 1991;349(6309):510-512.
31. Dias A, Ciminelli VST. Electroceramic Materials of Tailored Phase and Morphology by Hydrothermal Technology. Chem Mater. 2003;15(6):1344-1352.
32. Li Q, Newberg JT, Walter EC, Hemminger JC, Penner RM. Polycrystalline Molybdenum Disulfide (2H– MoS_2) Nano- and Microribbons by Electrochemical/Chemical Synthesis. Nano Lett. 2004;4(2):277-281.
33. Tenne R, Margulis L, Genut M, Hodes G. Polyhedral and cylindrical structures of tungsten disulphide. Nature. 1992;360(6403):444-446.
34. Zelenski CM, Dorhout PK. Template Synthesis of Near-Monodisperse 1 Microscale Nanofibers and Nanotubules of MoS_2. Journal of the American Chemical Society. 1998;120(4):734-742.
35. Tian Y, Zhao X, Shen L, Meng F, Tang L, Deng Y, et al. Synthesis of amorphous MoS_2 nanospheres by hydrothermal reaction. Mater Lett. 2006;60(4):527-529.
36. Nagaraju G, Tharamani CN, Chandrappa GT, Livage J. Hydrothermal synthesis of amorphous MoS_2 nanofiber bundles via acidification of ammonium heptamolybdate tetrahydrate. Nanoscale Research Letters. 2007;2(9).
37. Gray CT. Introduction to quality engineering: Designing quality into products and processes, G. Taguchi, Asian productivity organization, 1986. number of pages: 191. price: $29 (U.K.). Qual Reliab Eng Int. 1988;4(2):198-198.
38. Harris LN. Taguchi techniques for quality engineering, Philip J. Ross, Mcgraw-hill book company, 1988. Qual Reliab Eng Int. 1989;5(3):249-249.
39. Battered Women: A Psychosociological Study of Domestic Violence. Edited by Maria Roy. New York: Van Nostrand Reinhold Co., 1977. 334 pp. $10.95. Soc Work. 1978;23(4):341-341.
40. Tanaydin S, Park SH. Robust Design and Analysis for Quality Engineering. Technometrics. 1998;40(4):349.
41. Ma Y, Nie X, Northwood DO, Hu H. Systematic study of the electrolytic plasma oxidation process on a Mg alloy for corrosion protection. Thin Solid Films. 2006;494(1-2):296-301.
42. Berntsen N, Gutjahr T, Loeffler L, Gomm JR, Seshadri R, Tremel W. A Solvothermal Route to High-Surface-Area Nanostructured MoS_2. Chem Mater. 2003;15(23):4498-4502.
43. Albiter MA, Huirache-Acuña R, Paraguay-Delgado F, Rico JL, Alonso-Nuñez G. Synthesis of MoS_2 nanorods and their catalytic test in the HDS of dibenzothiophene. Nanotechnology. 2006;17(14):3473-3481.
44. Wang F, Li F, Zheng M, Li Y, Ma L. The rational design of hierarchical MoS_2 nanosheet hollow spheres sandwiched between carbon and TiO_2@graphite as an improved anode for lithium-ion batteries. Nanoscale Advances. 2019;1(5):1957-1964.